arXiv:nucl-ex/0408019v1 17 Aug 2004

# SEARCH FOR PENTAQUARK STATES WITH CLAS AT JEFFERSON LAB

V. D. BURKERT
*Jefferson Lab, 12000 Jefferson Avenue, Newport News VA 23606, USA*
*E-mail: burkert@jlab.org*

R. DE VITA
*Istituto Nazionale di Fisica Nucleare*
*via Dodecaneso 33, 16146 Genova, Italy*
*E-mail: devita@ge.infn.it*

S. NICCOLAI
*IPN Orsay,*
*15 rue Georges Clemenceau,*
*91406 Orsay France*
*E-mail: silvia@jlab.org*

AND THE CLAS COLLABORATION

We discuss the experimental program to search for baryon states with exotic flavor quantum numbers using CLAS at Jefferson Lab

## 1. Physics Motivation

The existence of baryons with quantum numbers that cannot be obtained with only 3 valence quarks $qqq$, but require a minimum quark content $qqqq\bar{q}$, has excited the hadron community since the first public announcements of such a state were made in the year 2003. The observed state is now called the $\Theta^+(1540)$. It appears to have a mass in the range 1525 MeV to 1550 MeV, and strangeness S=+1 [1]. While pentaquark states with such quantum numbers have been discussed for years, specific predictions for both a mass of 1530 MeV and a narrow width of $< 15$ MeV were made in a paper by Diakonov et al. in 1997 [2], based on the Chiral Soliton Model ($\chi SM$). In this model, the $\Theta^+$ is an isosinglet member of a $J = \frac{1}{2}^+$ anti-decuplet of ten states with a minimum quark content of 5 quarks ("pentaquarks"),

three of the states have exotic flavor quantum numbers, the $\Theta^+$, and the two baryons $\Xi_5^{--}$ and $\Xi_5^+$. The other non-exotic members are three $\Sigma_5$, and two $N_5^*$ states. The width appears to be much more narrow than the experimental resolutions, and may be as narrow as 1 MeV[3,4,5]. Following the first experimental announcements, an avalanche of theoretical papers have appeared trying to understand its low mass and narrow width, as well as to make predictions on production mechanism and possible excited states of the $\Theta^+$ [?,6]. Lattice QCD is currently not providing fully satisfactory predictions for the $\Theta^+$. One group finds no signal, three groups find a signal at about the right mass, two at negative parity, one at positive parity[7].

Evidence for the state has been claimed in more than 10 published works [8] from medium energy to very high energy experiments. There are a number of experiments, mostly at high energies, that report null results. Most of the results, if not all, come from the analysis of data that were taken for other purposes. This fact may explain the relatively low significance of all positive results, which ranges from about $4\sigma$ to $7\sigma$ for individual experiments. Experimentally, the $\Theta^+$ has been observed in either $nK^+$, or $pK^0$ final states. Reported masses in some cases vary by more than the uncertainties given for the individual experiments, with the masses obtained from processes involving $nK^+$ in the initial or final states giving on average 10-15 MeV higher masses. The discrepancy in mass determination needs to be resolved, but may not solely be an experimental problem. For example, the mass difference might be explained by different initial or final state interactions involved in $nK^+$ and $pK^0$ channels. Also, different interference effects could be involved that depend on the kinematics where the signal is observed. In either case theoretical input will be needed to resolve the discrepancy. Finding a definite answer to the question of existence or non-existence of the $\Theta^+$ and of the other 5-quark baryons is, of course, of overriding importance and urgency. It will tell us much about how QCD works at the hadron scale, and can only be answered experimentally.

In this contribution we report on the results from Jefferson Lab using the CLAS detector, and on the current program of second generation experiments aimed at improving the statistical accuracy of the measurements by at least one order of magnitude. We also need to better understand the systematics involved and obtain some insight into production mechanisms. In section 2 we report the experimental apparatus to the degree it is relevant for the physics at hand. In section 3 we discuss the already published results. Section 4 describes ongoing analyses, and in section 5 we report on the status of two second generation measurements, and then outline

planned experiments to further study the systematics of pentaquark states.

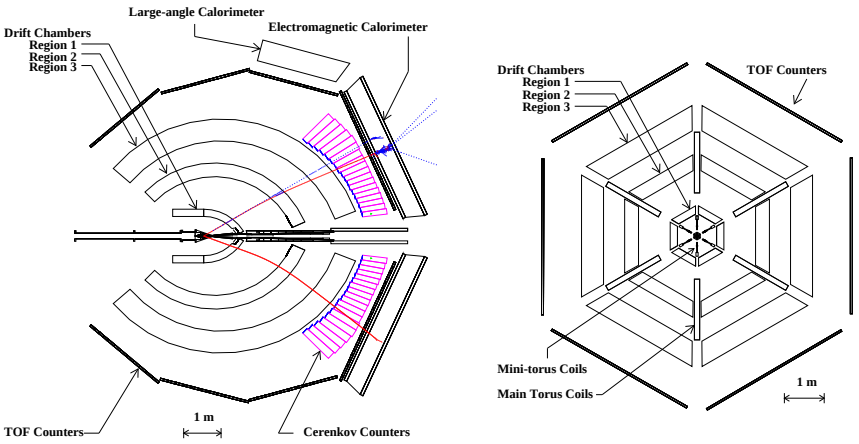


Figure 1. The CLAS detector. Left: Longitudinal cut along the beam line shows the 3 drift chamber regions, the Cherenkov counters at forward angles for electron and pion separation, the time-of-flight system, and the electromagnetic calorimeters for the detection of photons and neutrons. Right: Transverse cut through CLAS. The superconducting torus coils provide a six sector structure, each sector being instrumented with independent detectors.

## 2. CLAS and CEBAF - unique capabilities for baryon spectroscopy

The continuous electron beam provided by the CEBAF accelerator is converted into a bremsstrahlung photon beam at CLAS using a gold radiator located 20 meters upstream of a liquid hydrogen or deuterium target. The photon energy is measured by detecting the scattered the electrons that generated the photons in the energy range from 20% to 95% of the incident electron energy. Typical photon beam rates range from a few times $10^6$ to $10^7$ per second. The CLAS detector is shown in Fig. 1. At its core is a superconducting toroidal magnet, providing momentum analysis of charged particles in six sectors. The magnetic field produced by the six-coil toroidal magnet is oriented in such a way as to maintain a constant azimuthal angle of the scattered particles while changing only their polar angle. Tracking is provided with three regions of drift chambers with a total of 34 layers of drift cells arranged radially from the target. The total number of drift cells in CLAS is about 35,000 providing a highly redundant tracking infor-

mation. Charged tracks are reconstructed in polar angles from about 10 to 140 degrees. 288 plastic scintillator paddles provide time-of-flight information used for particle identification. For experiments with a bremsstrahlung photon beam, a segmented scintillation counter is arranged around the target for triggering and to provide improved start time information. CLAS is optimized for the selection of exclusive processes in a large kinematic range and with good resolution. The large acceptance of CLAS allows simultaneous measurement of several processes.

Often, as is also the case in the study of the $\Theta^+$, the missing mass technique is used to identify final states with one unmeasured particle, usually a neutron or a neutral meson. At intermediate energies all kinematic regions can play important roles, and may be sensitive to different production mechanisms, e.g. in s-channel, t-channel, and u-channel processes. With its large coverage CLAS can explore baryon excitation processes in all of these regions. These capabilities are unique to CLAS and, as long as the major production mechanisms are unknown, are crucial in the study of processes with small cross sections, such as the $\Theta^+$ or its possible excited states. For example, the small $\Theta^+$ signal may be completely swamped by background processes in t-channel kinematics. However, it may show up more prominently in u-channel kinematics through baryon exchange processes at large cms angles. The wide coverage of CLAS allows selection of all kinematics and reaction channels, and provides the utmost in sensitivity.

Table 1. Runs completed in Hall B at Jefferson Lab with the CLAS detector using photon beams. The experimental conditions are summarized.

| Experiment | Year | Beam Energy | Target | $\int \mathcal{L}$ (pb$^{-1}$) |
|---|---|---|---|---|
| g6a | 1998 | 4.1 GeV | $LH_2$ | $\sim 1.0$ |
| g6b | 1999 | 5.5 GeV | $LH_2$ | $\sim 1.0$ |
| g1c | 1999 | 1.9-3.1 GeV | $LH_2$ | $\sim 4.0$ |
| g6c | 2000 | 5.7 GeV | $LH_2$ | $\sim 2.7$ |
| g2a | 1999 | 2.5-3.1 GeV | $LD_2$ | $\sim 2$ |
| g3a | 1999 | 1.6 GeV | $L^3He$ | $\sim 0.3$ |

Since 1998, several experiments using photon beams and different targets have been completed: a summary is given in Table 1. In the last year, the existing CLAS data were reanalyzed to study possible evidence for pentaquark production. The CLAS collaboration has published two positive signals on the $\Theta^+$ using deuterium [14] and hydrogen targets [15]. We discuss these in the following section.

## 3. Discussion of published results

### 3.1. *Production on deuterium*

The first evidence for the $\Theta^+$ was seen in experiments on nuclear targets [12,13,14]. In CLAS, the fully exclusive process $\gamma D \to K^- p K^+ n$ was measured. The 4-momentum vectors of the photon, target nucleus, and all charged particles in the final state are known, the neutron can be identified by computing the missing mass of the remaining system as can be seen in Fig. 2. In this process the $\Theta^+$ would be produced on the neutron in the

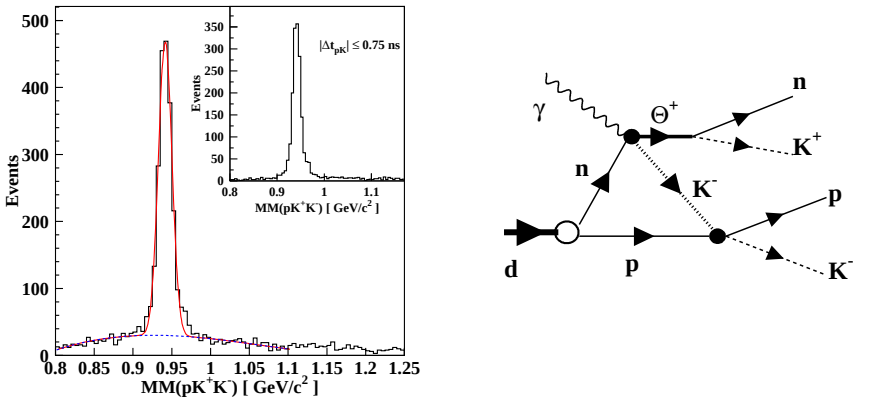


Figure 2. Left: Missing mass $M_X$ of $\gamma d \to p K^- K^+ X$. A peak at the neutron mass is seen. The inset shows the results with more stringent vertex time cuts. Right: Possible diagram for the observed process.

deuteron, while the proton would be a spectator. However, in order to be able to detect the proton in CLAS, it must have a minimum momentum of about 200 MeV/c. This requires a complex final state interaction. The final state also contains $\phi$ and $\Lambda(1520)$ that are eliminated by cuts in the $K^+K^-$ and $pK^-$ invariant mass spectra. A possible diagram is shown in Fig. 2. The final spectrum is shown in Figure 3. The $nK^+$ invariant mass shows a significant peak at $1542 \pm 5$ MeV. An analysis of these data using a different technique finds that the significance of the observed peak may not be as large as presented in the published work. We expect a definitive answer from a much larger statistics data set (g10) that is currently being analyzed.

.

Could this peak be generated by a statistical fluctuation? If we consider this result isolated from the evidence seen by other independent ex-

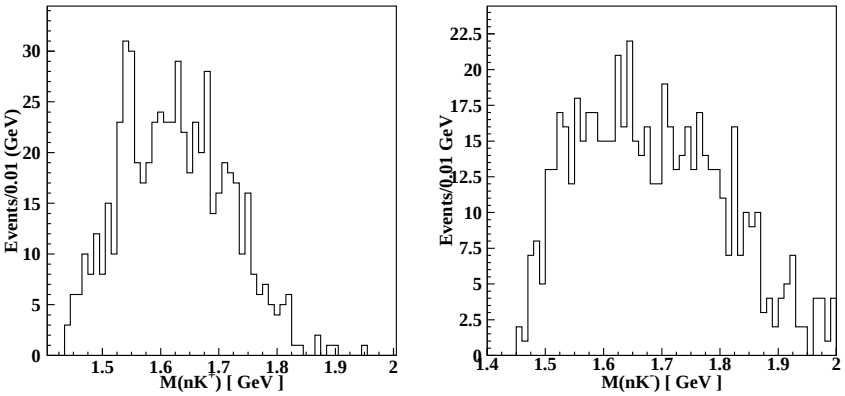


Figure 3. Left: Invariant mass distribution $M(nK^+)$ for the final state $pK^-nK^+$. Right:$M(nK^-)$ for the same event as in the left graph. The lack of a narrow peak shows that kinematic reflections do not seem to generate narrow structures in $nK^-$.

periments, there is a small probability that it could be a fluctuation. However, such an interpretation becomes extremely unlikely if the evidence from other independent experiments is considered. Other effects such as kinematical reflections have been studied. Here structures in (NK) mass spectra may be produced as kinematical reflections of high mass meson production with decays to the $K^+K^-$ final state. If the phase space for the reaction is limited, the invariant mass $nK^+$ could show an enhancement in the 1.55 GeV mass range. Kinematical reflections are well-known effects in spectroscopy, and have been studied extensively. For the current analysis, broad enhancements or shoulders can indeed be produced this way as is shown in the right panel of Fig. 3, where the mass of the $K^-n$ is shown using the same events that are included in the left panel. The smooth shoulder near 1.55 GeV may indeed be due to such an effect. Clearly, the sharp $\Theta^+$ peak in the left panel has very different characteristics from a kinematical reflection.

### 3.2. *Production on hydrogen*

Here the process $\gamma p \to \pi^+K^+K^-n$ is selected, using the g6a, g6b, and g6c data runs [15]. Cuts are applied with the hypothesis that the $\Theta^+$ is produced via intermediate $N^*$ excitation. Possible contributions to that channel are shown in Fig. 4. Events are selected with a forward angle $\pi^+$, and events with a forward angle $K^+$ are ejected. The latter cut was used to reduce t-channel contributions to $K^+$. The final mass spectrum is shown in Fig. 5.

A very significant peak is seen at a mass of $1.555 \pm 10$ MeV. In this analysis background processes contributing to the selected channel were subjected to a partial wave analysis. This allowed for a precise determination of the shape of the background contributions.

If the reaction mechanism is indeed through excitation of an intermediate $N^*$, then such a $N^*$ would presumably not be a usual 3-quark state but rather a 5-quark or even 7-quark state with strong $s\bar{s}$ components. Selecting events in the mass range around the peak, and plotting the invariant mass $nK^+K^-$ in Fig. 5 we see indications of a structure near 2.4 GeV. While the results hint at a narrow structure near 2.4 GeV the statistics are too poor to allow drawing definite conclusions. Further studies with higher statistics are clearly needed.

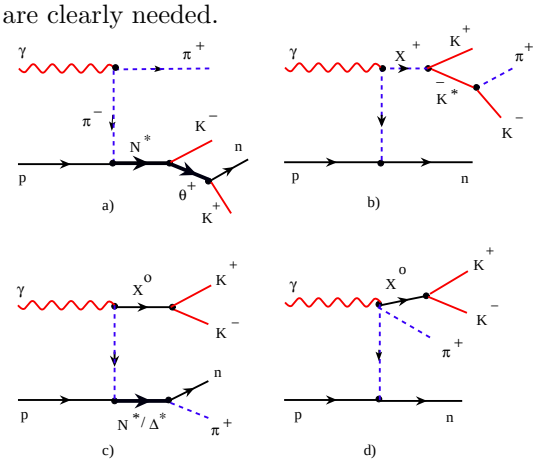


Figure 4. Diagrams that may contribute to the process $\gamma p \to \pi^+ K^- n K^+$. The left top diagram contributes to $\Theta^+$ production through intermediate $N^*$ excitation. The other diagrams represent background processes.

## 4. Ongoing analysis

*In this section we describe analyses that have shown some promise in the search for the $\Theta^+$ and possible excited states, however they lack the statistics and significance to be fully convincing. The CLAS collaboration has decided to not publish these works but wait for the completion of the ongoing runs with much higher statistics. Although no final results are presented here, it may be instructive to describe the techniques used in preparation for the analysis of the new high statistics data.*

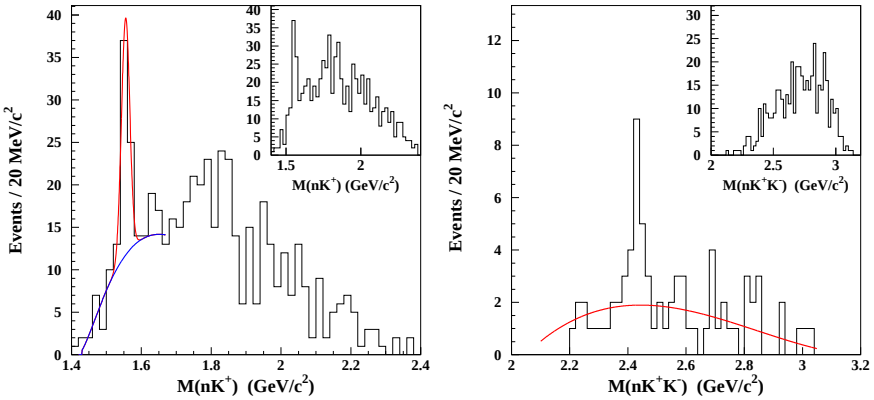


Figure 5. Left: Invariant mass distribution of $M(nK^+)$ after all cuts. The inset shows the $nK^+$ mass distribution with only the $\cos\theta^*_{\pi^+} > 0.8$ cut applied. Right: Mass distribution $M(K^-nK^+)$ for events selected in the peak region of the graph on the left. The inset shows the distribution for events outside of the $\Theta^+$ region.

### 4.1. *Reactions on protons*

The $g1c$ data set was used to study the reaction $\gamma p \to K^+\bar{K}^0 n$ and $\gamma p \to pK^+K^-$, searching for evidence of $S = +1$ resonances in the $K^+n$ and $K^+p$ invariant masses.

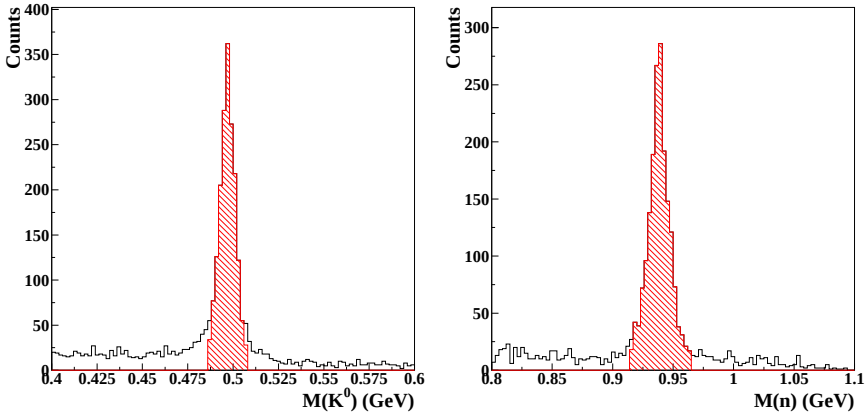


Figure 6. Final particle identification for the reaction $\gamma p \to K^+\bar{K}^0 n$. The left plot shows the $\bar{K}^0$ mass spectrum reconstructed as invariant mass the $\pi^+\pi^-$ system. The right plot shows the $K^+\pi^+\pi^-$ missing mass.

The first channel was selected by detecting the $K^+$ and reconstructing the $\bar{K^0}$ via the $K_s$ component decaying into $\pi^+\pi^-$. The final state was then identified using the missing mass technique. Figure 6 shows the quality of the channel identification: both $\bar{K^0}$ and $n$ are reconstructed within 1-2 MeV of the nominal mass value with small background. The corresponding event sample is dominated by the production of known hyperons decaying into the same final state. These include $\gamma p \to K^+\Lambda^*(1520)$, $\gamma p \to K^+\Sigma^+\pi^-$, and $\gamma p \to K^+\Sigma^-\pi^+$. Fig. 7 shows the $\Lambda^*(1520)$ and $\Sigma^+$ peaks reconstructed as missing mass of $K^+$ and the $K^+\pi^-$ system. Events associated with these reactions are excluded by cutting on the corresponding masses. After such cuts, the $nK^+$ invariant mass spectrum was constructed. After selecting events in which the $\bar{K^0}$ is emitted at backward angles, two structures with masses near $\sim 1525$ and $\sim 1575$ MeV were visible. However, the low statistics of the final event sample did not allow us to draw definitive conclusion on such structures.

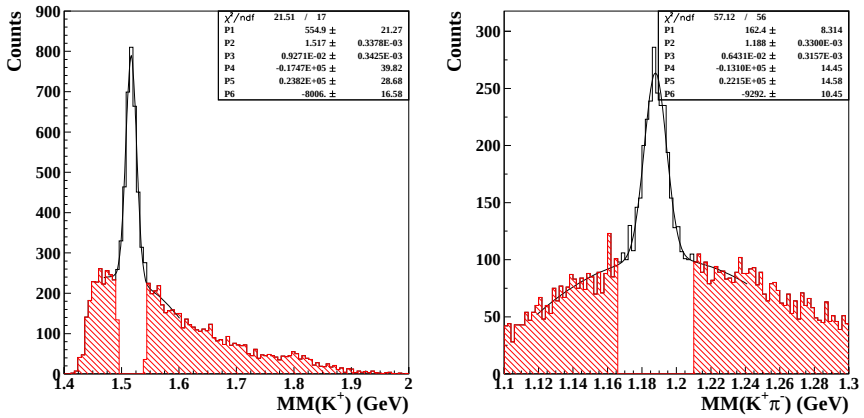


Figure 7. $K^+$ and $K^+\pi^-$ missing masses after the cuts on the $K^+$ and $\bar{K^0}$, and $n$ masses. The $\Lambda^*(1520)$ and $\Sigma^+$ peaks are clearly visible. The highlighted areas correspond to the events selected for further analysis.

The reaction $\gamma p \to pK^+K^-$ was selected by detecting two of the three charged particles in CLAS and using the missing mass technique allows us to identify the third one. Two different topologies, $\gamma p \to pK^+(K^-)$ and $\gamma p \to (p)K^+K^-$, were analyzed while the topology with $pK^-$ detected was dropped due to the marginal statistics. One of the largest contributions to

this particular final state is due to the diffractive production of the $\phi(1020)$ meson. This is shown in the left panel of Fig. 8. The associated events as well as the events coming from $\Lambda^*(1520)$ production (see the right panel of the same figure) are rejected by cutting on the corresponding masses. To further reduce the background contribution coming from other reactions and to maximize the signal to background ratio, angular and energy regions were selected where Monte Carlo simulations showed maximum sensitivity to the reactions of interest. After these additional cuts, the $pK^+$ invariant mass spectrum showed a structure in the mass region around 1.58 MeV. However also in this case, the limited statistics did not allow us to reach definitive conclusions.

In either case, the much higher statistics of the g11 experiment that will finish data taking by July 29, 2004, will allow more definite conclusions as to the existence and significance of these possibly new narrow structures.

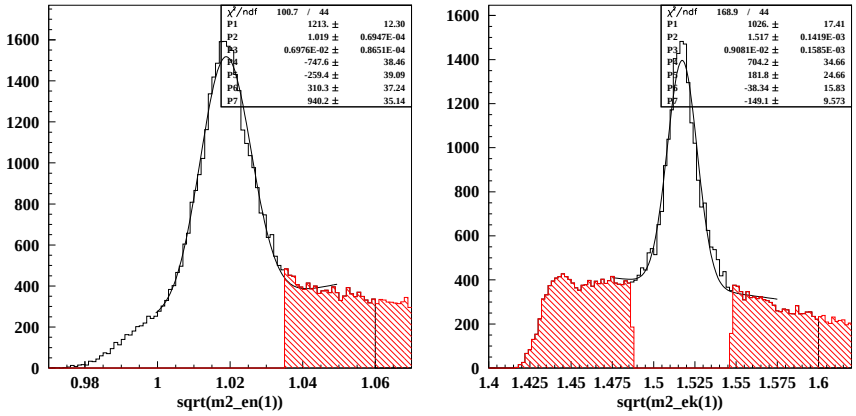


Figure 8. $p$ and $K^+$ missing masses showing the $\phi(1020)$ and $\Lambda^*(1520)$ contribution. The highlighted areas correspond to the events selected for further analysis.

### 4.2. *Reactions on $^3He$*

The $g3c$ data set was analyzed searching for the reaction $\gamma^3\mathrm{He} \rightarrow p\Lambda\Theta^+$. The advantage of this channel (see [16] for theoretical predictions of the cross section) is that it allows to identify the final state without the need of cutting on competing channels, while at the same time excluding kinematical reflections in the $NK$ invariant mass spectrum. Moreover, thanks to the

presence of the $\Lambda$ having strangeness $S = -1$, the $pK^0$ decay mode must have $S = +1$. The reaction threshold is $E_\gamma \simeq 800$ MeV for a $\Theta^+$ mass of 1.55 GeV/c$^2$. The main reaction mechanism can be pictured as a two-step process (Fig. 9): the initial photon interacts with one of the protons of $^3$He and produces a $\Lambda$ and a $K^+$ ($\gamma p \to K^+\Lambda$). The $\Lambda$ leaves the target nucleus, while the $K^+$ reinteracts with the neutron in $^3$He to form a $\Theta^+$. In this process, one of the two protons of $^3$He can either be a spectator, as pictured in Fig. 9, or rescatter, and thus gain enough momentum to be detected.

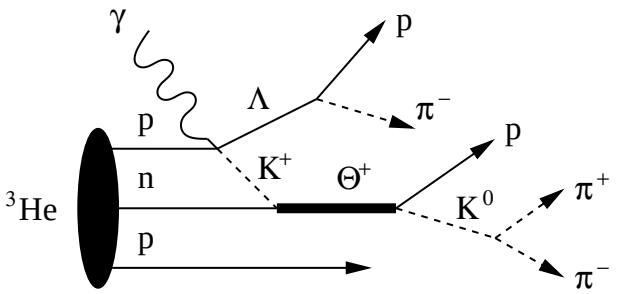


Figure 9. Production mechanism for $\Lambda\Theta^+$ in $^3$He. The decay modes $\Lambda \to p\pi^-$, $\Theta^+ \to K^0 p$ and $K^0 \to \pi^+\pi^-$ are shown here.

The following decay channels are most suitable for detection in CLAS:

- $\Lambda \to p\pi^-$,
- $\Theta^+ \to pK^0$ and $\Theta^+ \to nK^+$,
- $K^0 \to \pi^+\pi^-$.

The final state therefore is $p\pi^-p\pi^+\pi^-p$ for the $\Theta^+ \to pK^0$ decay mode, and $pp\pi^-nK^+$ for the $\Theta^+ \to nK^+$ decay mode. Having many particles in the final state (6 for the $\Theta^+ \to pK^0$ case, 5 for the $\Theta^+ \to nK^+$ case), many different topologies of detected particles in the final state are possible. The most promising three techniques are summarized in Table 2.

Event selections in the 3 analyses are shown in Figs. 10, 11, 12. In all three cases the final state is well identified, without the need of applying cuts to remove background channels.

The preliminary analysis reveals an enhancement in the $NK$ invariant mass spectrum, near 1.55 GeV/c$^2$. While the statistical significance of the peak is limited, this analysis shows that a search for the $\Lambda\Theta^+$ channel can contribute towards resolving the issue of the $\Theta^+$. The final state can be identified, unambigously, and no kinematical reflections can produce peaks

Table 2. Decay modes, combinations of detected particles in the final state and channel-identification techniques adopted for the analysis of the $\gamma^3$He$\rightarrow p\Lambda\Theta^+$ reaction.

| Decay modes | Final-state particles | Channel ID |
|---|---|---|
| $\Theta^+ \rightarrow pK^0$, $\Lambda \rightarrow p\pi^-$ | $pp\pi^-\pi^+X$ | $m_X = m_\Lambda$<br>$m(\pi^-\pi^+) = m_{K^0}$ |
| | $pp\pi^-\pi^+\pi^-X$ | $m_X = m_p$<br>$m(p\pi^-) = m_\Lambda$<br>$m(\pi^-\pi^+) = m_{K^0}$ |
| $\Theta^+ \rightarrow nK^+$, $\Lambda \rightarrow p\pi^-$ | $pp\pi^-K^+X$ | $m_X = m_n$<br>$m(p\pi^-) = m_\Lambda$ |

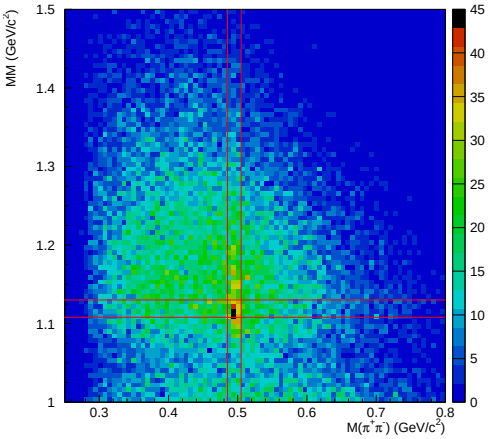


Figure 10. Analysis of the $pp\pi^+\pi^-$ topology. The cuts $E_\gamma > 1$ GeV and $p_p < 0.8$ GeV/c have been applied in order to reduce the background under the $\Lambda$ peak. Shown is here the missing mass of the $pp\pi^+\pi^-$ system as a function of the invariant mass of $\pi^+\pi^-$, the lines represent the cuts applied to select the $\Lambda$ (horizontal lines) and the $K^0$ (vertical lines)

in the $NK$ invariant mass distribution. An analysis of this reaction using the high-statistics photoproduction data on the deuteron (part of the g10 run) will give a more definite answer as to the existence and the properties of the $\Theta^+$ exotic baryon.

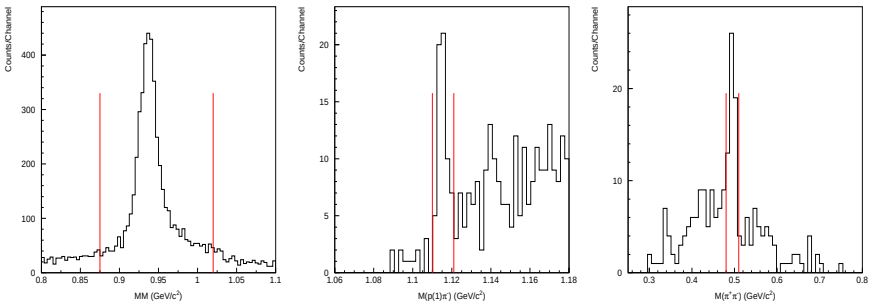


Figure 11. Results of the analysis for the $pp\pi^-\pi^+\pi^-$ topology. Left: missing mass of the $pp\pi^-\pi^+\pi^-$ system, showing a peak a the proton mass; center: invariant mass of the $p\pi^-$ system, peaking at the $\Lambda$ mass; right: invariant mass of the $\pi^+\pi^-$ system, the peak is at the $K^0$ mass. The vertical lines represent the selection cuts applied.

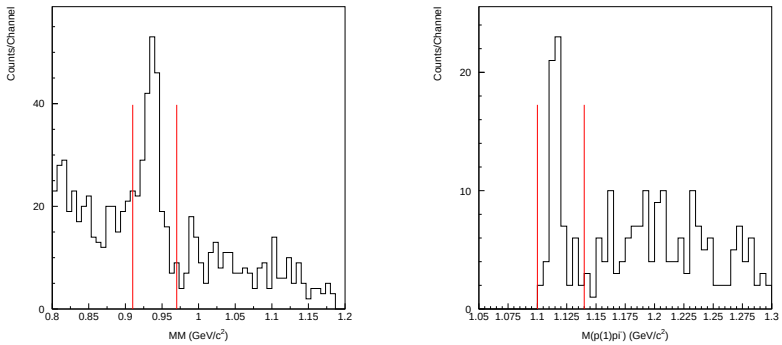


Figure 12. Results of the analysis for the $pp\pi^-K^+$ topology. Left: missing mass of the $p\pi^-K^+$ system, showing a peak at the neutron mass; right: invariant mass of the $p\pi^-$ system, peaking at the $\Lambda$ mass. The vertical lines represent the selection cuts applied.

## 5. Perspectives

The analysis of existing data shows the capabilities of CLAS to select exclusive final states with high multiplicity. The reaction channels described above were cleanly identified with small background due to misidentified particles. Concurrent reactions decaying to the same final states were seen and rejected from the final event sample. However the statistical accuracy of the preliminary data is not sufficient to exclude that the observed signals are due to statistical fluctuations, kinematic reflections, or some experimental artifact. The number of events in the $\Theta^+$ peaks is rather small and does

not allow us to perform detailed checks of systematic dependencies.

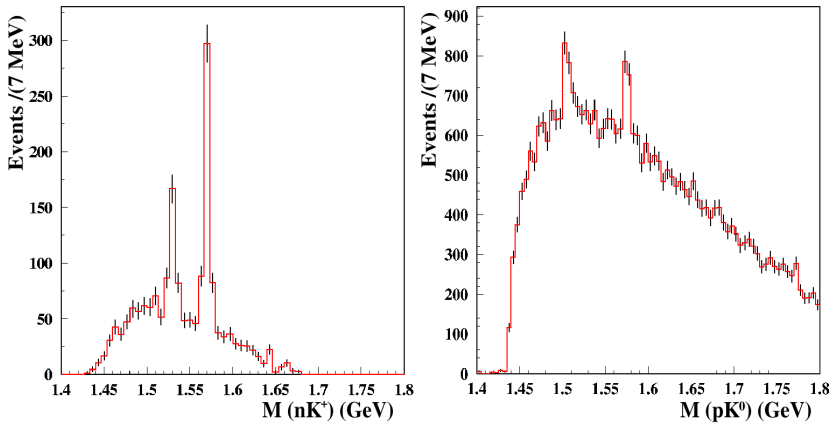


Figure 13. Expected statistical accuracy of the mass spectra for the reactions $\gamma p \to \Theta^+(\Theta^{+*})\bar{K}^0$, with $\Theta^+(\Theta^{+*})$ decaying into $K^+n$ (left) and $pK^0$ (right).

To obtain a definitive answer on the existence of pentaquark states, four dedicated experiments were recently approved for CLAS in Hall B at Jefferson Lab. The goals and experimental conditions of these experiments are summarized in Table 3.

Table 3. New experiments proposed in Hall B for the search of pentaquark states .

| Run | Beam | Energy | Target | Reaction | Status |
|---|---|---|---|---|---|
| g10 | $\gamma$ | 3.8 GeV | $LD_2$ | $\gamma d \to \Theta^+ K^- p$<br>$\gamma d \to \Theta^+ \Lambda^0$ | Completed |
| g11 | $\gamma$ | 4.0 GeV | $LH_2$ | $\gamma p \to \Theta^+ \bar{K}^0$<br>$\gamma p \to \Theta^+ K^- \pi^+$ | In progress |
| eg3 | $e$ | 5.7 GeV | $LH_2$ | $\gamma_v p \to \Xi^{--} X$<br>$\gamma p \to \Xi^+ X$ | December 2004 |
| g12 | $\gamma$ | 5.7 GeV | $LH_2$ | $\gamma p \to \Theta^+ K^- \pi^+$<br>$\gamma p \to \Theta^+ \bar{K}^0$<br>$\gamma p \to K^+ K^- \Xi^-$ | To be scheduled |

### 5.1. *Search for the $\Theta^+$ and excited states*

The g10 experiment [17], which has taken data during the spring of 2004, aims at studying the production channels $\gamma d \to pK^-\Theta^+$, $\gamma d \to pK^0X$, and

$\gamma d \to \Lambda\Theta^+$ with an order of magnitude improved statistics over the previous g2a run. The g11 experiment will study $\gamma p \to \Theta^+ \bar{K}^0$ and $\gamma p \to \Theta^+ K^- \pi^+$, and two decay modes, $\Theta^+ \to nK^+$ and $\Theta^+ \to pK^0$, increasing by an order of magnitude the statistics of the previous data. Both experiments have similar experimental setups and beam condition as used in the g2a and g1c runs, respectively. The g11 experiment [18] will use tagged photons produced from a 4 GeV primary electron beam impinging on a 40-cm long hydrogen target. Photons from 1.6 GeV up 3.8 GeV are tagged and the data acquisition is triggered by events with at least two tracks to maximize the efficiency for the reaction of interest. The total expected integrated luminosity is 75 pb$^{-1}$, i.e. approximately 20 times larger than in the previous run.

If the $\Theta^+$ can be established with certainty, the new data will allow us to make progress on establishing the phenomenology of the $\Theta^+$ spectrum, e.g. determining in what production channels the $\Theta^+$ is seen and what higher mass states are excited. The expected statistical accuracy is shown in Fig. 13, where the background was estimated based on the existing data and the signal was simulated assuming a production cross section of $\sim 10$ nb. If the existence of the $\Theta^+$ is confirmed or new states are seen, these data will provide accurate measurements of the mass position. In addition, the large acceptance of the CLAS detector will allow us to measure both the production and decay angular distribution, providing information on the production mechanism and spin. Expected statistical accuracy for the measurement of the production and decay angular distributions are shown in Fig 14, for different assumptions on the production angular distribution and for the spin and parity of the pentaquark state.

This measurement will provide a solid foundation for a long term plan for the investigation of the pentaquark spectrum and properties.

### 5.2. *Search for $\Xi_5^{--}$ and $\Xi_5^-$ baryons.*

The anti-decuplet predicted by the $\chi SM$ or quark-cluster models [19,20] for 5-quark states also contains $\Xi_5$ states, two of them of exotic nature, the $\Xi_5^{--}$ and the $\Xi_5^+$. Evidence for such states has so far been seen in only one experiment [23]. The signal found by NA49 has a mass 100 to 200 MeV away from any prediction. This makes it urgent to confirm or refute these claims. Two new experiments with CLAS are in preparation to search for $\Xi_5$ baryons.

The eg3 experiment [22] will use an untagged electron beam of 5.75 GeV

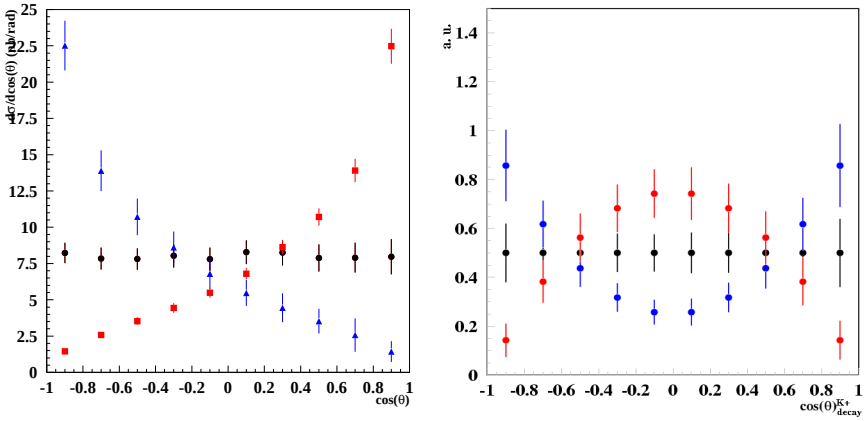


Figure 14. Expected statistical accuracy for the measurement of the production and decay angular distribution. A total cross section of $\sim$ 10 nb was assumed. The left plot shows the expected error bars for the production angular distribution in the assumption of a t-channel, s-channel, and u-channel production mechanism. The right plot shows the expected error bars for the decay angular distribution for different assumption on the spin and parity of the state and 100% polarization.

impinging on a liquid-deuterium target. Electrons will interact with the neutrons in the deuterium through exchange of quasi-real photons. The process $\gamma^* n \rightarrow \Xi^{--} X$ will be searched for by measuring the decay chain $\Xi^{--} \rightarrow \pi^- \Xi^- \rightarrow \pi^- \Lambda \rightarrow \pi^- p$. One proton and 3 $\pi^-$ emerging from three different vertices have to be reconstructed. The experiment is scheduled to take data in the winter 2004/2005.

The second experiment [21] is part of g12. It uses the missing mass method to search for the $\Xi^-$ in the exclusive reaction $\gamma p \rightarrow K^+ K^+ X$. If the NA49 results are correct, the $\Xi^-$ would be seen in the missing mass spectrum as a peak at 1862 MeV. Excellent missing mass resolution is required for such a measurements. Figure 15 illustrates the method with data taken at photon energies between 3.2 - 3.9 GeV. The $\Xi(1320)$ ground state is observed as a narrow spike. Limitations in beam energy and/or in the statistics did not allow us to observe higher mass $\Xi' s$ in this measurement.

## 6. Summary

In conclusion, CLAS is currently pursuing high statistics searches for the $\Theta^+$ on hydrogen and deuterium, and in various final states. We are also searching for possible excited states of the $\Theta^+$. The experiments are con-

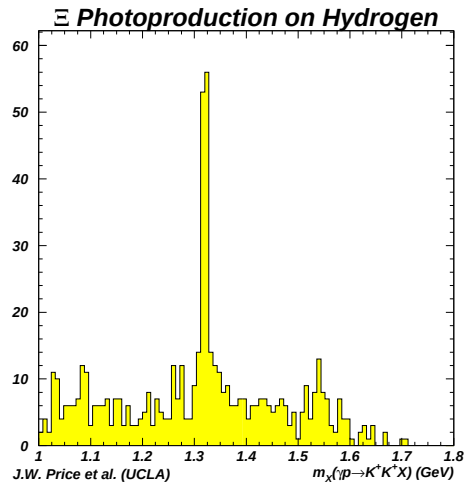


Figure 15. Missing mass $M_X$ for the reaction $\gamma p \rightarrow K^+K^+X$ for photon energies in the range 3.2 to 3.9 GeV. The narrow peak observed for the ground state $\Xi(1320)$ illustrates the excellent mass resolution that can be obtained using this method [21]. For the pentaquark $\Xi_5$ search, higher energies and much higher statistics are needed.

ducted under similar kinematical conditions as previous measurements. The much higher statistics will allow more definite conclusions as to the existence of the $\Theta^+$ in the exclusive channel $\gamma d \rightarrow K^-pK^+(n)$. In addition, the existence of a possible excited state with mass about 50 MeV above the $\Theta^+$ will be clarified. Moreover, an experiment is in preparation to search for the $\Xi_5^{--}$ in the mass range where the NA49 experiment at CERN claimed evidence for the observation of the $\Xi_5(1862)$ in various charge channels. If evidence for the pentaquark states remains and is considerably strengthened, another high statistics experiment (g12) will be able to study the spectroscopy of pentaquark states.

## 7. Acknowledgments

This work was supported by the Italian Istituto Nazionale di Fisica Nucleare, the French Centre National de la Research Scientifique, the French Commissariat à l'Energie Atomique, the U.S. Department of Energy, the U.S. National Science Foundation, and the Korean Science and Engineering Foundation. The Southeastern Universities Research Association (SURA) operates the Thomas Jefferson National Accelerator Facility for the United States Department of Energy under contract DE-AC05-84ER40150.

## References

1. For recent experimental overviews see: T. Nakano, these proceedings.
2. D. Diakonov, V. Petrov, and M. Polyakov, Z. Phys. A359, 305 (1997).
3. R. Arndt et al., Phys. Rev. C68, 42201 (2003).
4. C. Cahn and G. Trilling, Phys. Rev. D69, 011501 (2004).
5. W. Gibbs, nucl-th/0405024 (2004).
6. For a theoretical overviews see: M. Oka, hep-ph/0406211
7. F. Csikor, Z. Fodor, S.D. Katz, T.G. Kovacs, hep-lat/0407033; T.G. Kovacs, these proceedings.
8. K. Hicks, hep-ph/0408001.
9. J. Dudek and F. Close, Phys. Lett. B583, 278 (2004).
10. D. Borisyuk et al., hep-ph/0307370 (2003).
11. B. Mecking *et al.*, Nucl. Instr. and Meth. A503, 513 (2003).
12. T. Nakano et al., Phys. Rev. Lett. 91, 012002 (2003).
13. Dolgolenko et al., Phys. Atom. Nucl. 66, 1715 (2003).
14. S. Stepanyan et al. (CLAS collaboration), Phys. Rev. Lett. 91, 252001 (2003).
15. V. Koubarovsky et al., Phys.Rev.Lett. 92, 032001 (2004).
16. V. Guzay, hep-ph/0402060 (2004).
17. K. Hicks, S. Stepanyan, et al. (CLAS), Jlab experiment E-03-113.
18. M. Battaglieri, R. De Vita, V. Koubarovsky, et al. (CLAS), JLab experiment E-04-021.
19. R. Jaffe and F. Wilczek, Phys. Rev. Lett. 91, 232003 (2003).
20. M. Karliner and H. Lipkin, Phys. Lett. B575, 249 (2003).
21. J. Price, D. Weygand, et al. (CLAS), Jlab experiment E-04-017.
22. E. Smith, R. Gothe, S. Stepanyan, et al. (CLAS), JLab experiment E-04-010.
23. C. Alt et al. (NA49 collaboration), Phys. Rev. Lett. 92, 042003 (2004).